論文 Estimation of Friction Force Characteristics between Tire and Road Using Wheel Velocity and Application to Braking Control*

沢田　護　小野英一　浅野勝宏　菅井　賢
Mamoru SAWADA　Eiichi ONO　Katsuhiro ASANO　Masaru SUGAI
伊藤祥司　山本真規　安井由行
Shoji ITO　Masaki YAMAMOTO　Yoshiyuki YASUI

In order to improve the performance of a vehicle baking control, it is important to estimate friction force characteristics between tire and road. In this paper, an estimation method which estimates parameters concerned with friction force margin is proposed by applying the on-line least squares method to wheel rotational velocities. Then, the braking control using estimated parameters is proposed. The control aims at constant μ rate (i.e. generated friction force / maximum friction force) in order to improve vehicle braking and steering maneuvers. The effect of the control is shown by experiments.

Key words : Vehicle dynamics, Least-squares estimation, Brakes, Tires, Friction, Control

1. INTRODUCTION

The friction force characteristics of vehicle tires are changed depending on driving conditions. Then, robust control approach, which treats changes of tire characteristics as plant perturbations, is a proper method of vehicle control.[1] However, in order to achieve maximum performance of vehicles, it is necessary to estimate friction force characteristics of tire. There are various models describing friction force characteristics,[2) 3)] however, it is difficult to estimate the parameters of such models by using on-line identification methods.

In this paper, we estimate the slope of friction force against slip velocity at the operational point, or Extended Braking Stiffness (hereafter "XBS") as an important parameter describing friction force of tire. Maximum braking force can be obtained at the point XBS = 0 (see **Fig. 1**), and a decrease in XBS indicates a decrease in the margin of friction force. Then, the method brings high performance vehicle braking control which cannot be achieved by the robust control approach.

In the following sections, we propose the estimation method of XBS from wheel velocity by applying the on-line least squares method. Further, the braking control strategy based on estimated XBS is proposed, and high performance of the braking control is shown by experiments.

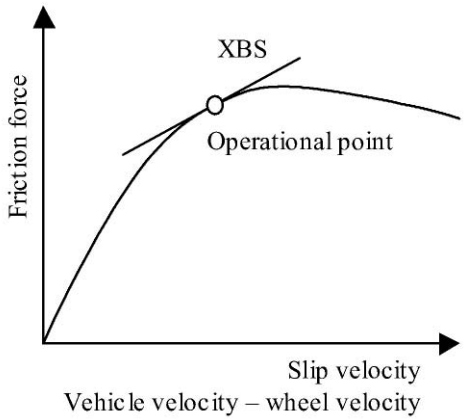

Fig. 1 Tire/road characteristics and extended braking stiffness (XBS)

2. ESTIMATION OF EXTENDED BRAKING STIFFNESS (XBS)

2.1 Wheel deceleration model

The pneumatic tires of the vehicle have rotational resonance from the wheel inertia and the sidewall spring.[4] However, the resonance vanishes when braking because of brake pad friction. Then, the rotational dynamics of the wheel (see **Fig. 2**) are modeled by the equation

$$J\dot{v}_w = r^2 F_x - rT + r^2 d, \qquad (1)$$

where,

J : moment of inertia of wheel,

＊（社）自動車技術会の了解を得て，「Proceedings of AVEC' 02」より転載

r : radius of wheel,

F_x : friction reaction force between tire and road,

T : brake torque (in proportion to wheel cylinder pressure),

d : disturbance from road, and

v_w : wheel velocity.

By assuming that vehicle dynamics are sufficiently slower than wheel dynamics and Fx is a function of slip velocity, the Wheel Deceleration Model can be obtained from (1).

$$\ddot{v}_w = -\frac{kr^2}{J}\dot{v}_w + w \qquad (2)$$

Here,

k : Extended Braking Stiffness (XBS),

w : disturbance from road and brake torque fluctuations ($w = r^2\dot{d} - r\dot{T}$).

If we assume constant deceleration braking, for example, μ-peak braking on constant μ road, brake torque T can be treated as a disturbance by differentiating (1). This implies that XBS can be estimated from wheel velocity. It is not necessary to use the wheel cylinder pressure value. (2) describes the dynamics of wheel deceleration, and XBS is proportionate to the break point frequency of the wheel deceleration model. Then, XBS can be estimated by identifying the break point frequency of (2).

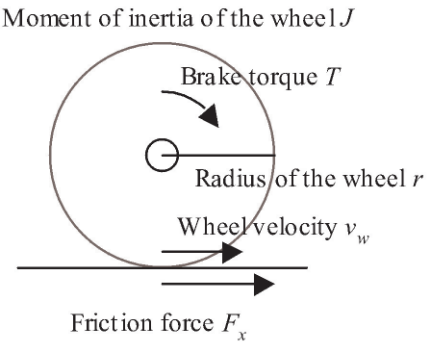

Fig. 2 Rotational dynamics of the wheel

Figure 3 shows experimental results of the vehicle braking with constant wheel cylinder pressure on packed snow road. While there is sufficient margin of friction force in **Fig. 3** (a), it shows critical braking near μ-peak in **Fig. 3** (b).

Figure 4 shows the experimental results of the frequency characteristics of wheel velocity shown in **Fig. 3** during braking. The magnitude of power spectrum density in low frequency increases according to the increase in wheel cylinder pressure, and break point frequency shifts to the left (low frequency). This indicates that XBS decreases according to the decrease in margin of friction force.

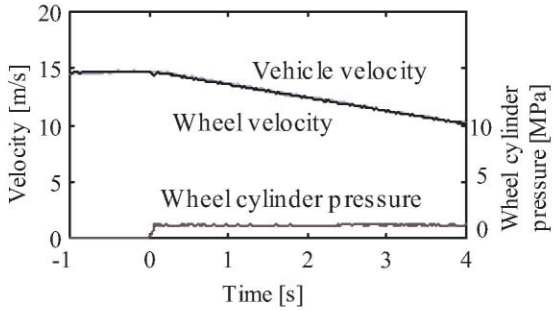

(a) Soft braking: Wheel cylinder pressure = 1MPa

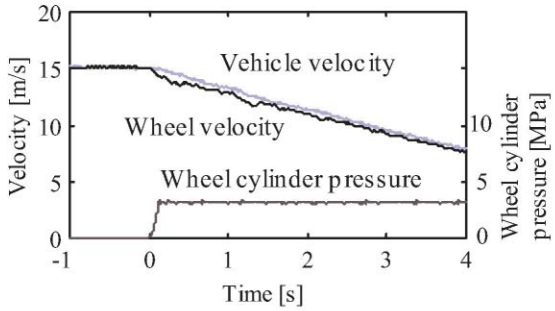

(b) Hard braking: Wheel cylinder pressure = 3MPa

Fig. 3 Experimental results of the vehicle braking with constant wheel cylinder pressure on packed snow road

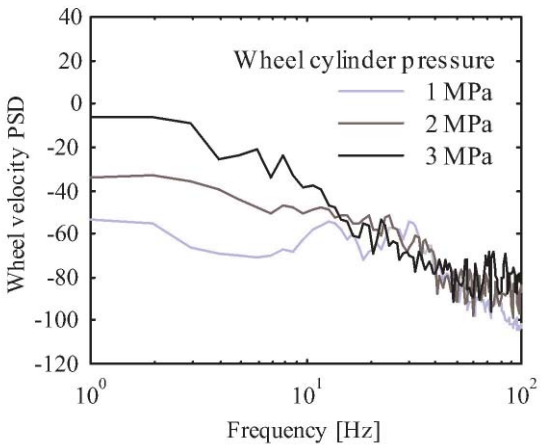

Fig. 4. Experimental results of the frequency characteristics of wheel velocity with constant wheel cylinder pressure on packed snow road. Hard braking: wheel cylinder pressure = 3 MPa (Fig. 3 (b)), moderate braking: wheel cylinder pressure = 2 MPa, soft braking: wheel cylinder pressure = 1 MPa (Fig. 3 (a))

2.2 Applying on-line least squares method

By assuming that w is white noise, XBS k can be estimated by applying the least squares method[5] to (2) as follows :

$$\phi[i]=\frac{\tau r^2}{J}\left(v[i-1]-v[i-2]\right) \quad (3)$$

$$y[i]=-v[i]+2v[i-1]-v[i-2] \quad (4)$$

$$L[i]=-\frac{P[i-1]\phi[i]}{\lambda+\phi[i]^2 P[i-1]} \quad (5)$$

$$P[i]=-\frac{1}{\lambda}\left[P[i-1]-\frac{\phi[i]^2 P[i-1]^2}{\lambda+\phi[i]^2 P[i-1]}\right] \quad (6)$$

$$\hat{k}[i]=\hat{k}[i-1]+L[i]\left(y[i]-\phi[i]\hat{k}[i-1]\right) \quad (7)$$

Here,

τ : sampling time,

ν : filtered (2-20 Hz band pass) wheel velocity,

$\hat{k}$: estimated XBS, and

λ : forgetting factor.

The algorithm described by (3)-(7) estimates XBS from the fluctuation phenomenon of wheel velocity. **Figure 5** shows estimated XBS by (3)-(7) of the experimental result shown in **Fig. 3** (b). XBS is on the decrease according to hard braking.

Figure 6 shows the relation between averaged XBS during braking and wheel cylinder pressure. According to the decrease in margin of friction force on each road surface, estimated XBS is on the decrease. This implies that the maximum braking force on each road surface can be obtained by the XBS servo control, i. e., actuation of wheel cylinder pressure which controls estimated XBS to the small value.

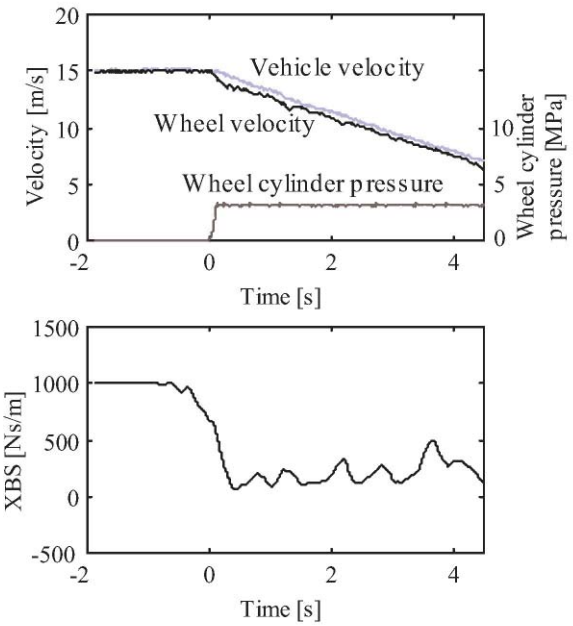

Fig. 5 Estimated XBS by (3)-(7) of the experimental results shown in Fig. 3 (b)

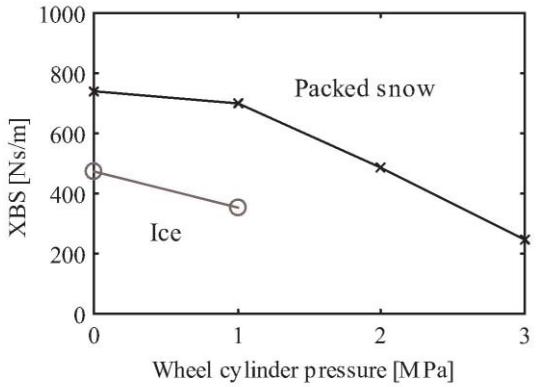

Fig. 6 Relation between averaged XBS during braking and wheel cylinder pressure

3. APPLICATION TO BRAKING CONTROL

The estimated XBS can be applied for brake controls, e.g. ABS. In this paper, we propose the brake control which obtains a constant μ rate in order to improve vehicle braking and steering maneuvers. For an experimental vehicle, a conventional ABS actuator and pressure sensor of the wheel cylinder are used for braking control. However, the conventional on-off ABS valves may not be suitable for the proposed system. Therefore, we only evaluate ABS performance such as stopping distance, steerability and stability. Noise and vibration due to the conventional ABS valves are not evaluated.

3.1 Control system structure

A control system to follow the reference value of XBS (XBS servo control) is realized by a 3 layered hierarchy control as shown in **Fig. 7**. In order to follow the reference of XBS, the XBS servo calculates the reference value of wheel deceleration, the deceleration servo calculates the reference value of the pressure of the wheel cylinder, and the brake servo calculates the valve command of ABS.

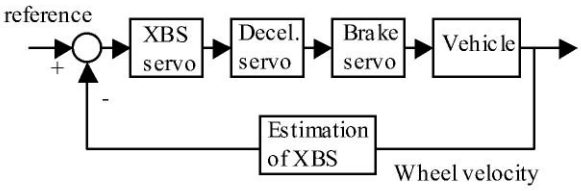

Fig. 7 Control system structure of XBS servo

3.2 XBS servo control

The XBS servo calculates the reference value of wheel deceleration in order to follow the reference of XBS. The reference of XBS is determined as follows.

Friction force characteristics during combined steering and braking maneuvers are described by the brush model.[2] In this paper, the following variables are defined in order to simplify the model.

$$\kappa_x = \frac{s}{1-s} = \frac{v_x - v_w}{v_w} \tag{8}$$

$$\kappa_y = \frac{K_\beta v_y}{K_s v_w} \tag{9}$$

$$\kappa = \sqrt{\kappa_x{}^2 + \kappa_y{}^2} \tag{10}$$

Here,

s : slip rate,
v_x : longitudinal velocity of wheel,
v_y : lateral velocity of wheel,
K_s : longitudinal stiffness of tire, and
K_β : lateral stiffness of tire.

Assuming that the direction of the friction force θ coincides with the slip direction, as

$$\tan\theta = \frac{\kappa_x}{\kappa_y}, \tag{11}$$

the friction force can be described as follows.

Case 1: $\xi_s = 1 - \dfrac{K_s}{3\mu F_z}\kappa > 0$

$$F_x = \mu F_z \cos\theta\left(1 - \xi_s{}^3\right) \tag{12}$$

$$F_y = \mu F_z \sin\theta\left(1 - \xi_s{}^3\right) \tag{13}$$

Case 2: $\xi_s = 1 - \dfrac{K_s}{3\mu F_z}\kappa < 0$

$$F_x = \mu F_z \cos\theta \tag{14}$$

$$F_y = \mu F_z \sin\theta \tag{15}$$

Here,

μ : maximum friction coefficient,
F_x : longitudinal friction force,
F_y : lateral friction force, and
F_z : load force.

Further, we define μ rate (i.e. generated friction force / maximum friction force) as

$$\gamma = \frac{F}{\mu F_z} = \frac{\sqrt{F_x{}^2 + F_y{}^2}}{\mu F_z}. \tag{16}$$

From (8)-(16), the slope of friction force F against slip κ can be described using γ $(0 \le \gamma < 1)$ as

$$\frac{\partial F}{\partial \kappa} = K_s\left(1-\gamma\right)^{\frac{2}{3}} \tag{17}$$

$\partial F/\partial k$ is described as a function of K_s and γ. This means that a constant μ rate is obtained by a control which gives a constant $\partial F/\partial k$, even if the maximum friction coefficient μ changes. Furthermore, XBS k can be described as

$$k = \frac{\partial F_x}{\partial \kappa_x}\cdot\frac{1}{v_w} = \frac{K_s}{v_w}\left[\left(1-\gamma\right)^{\frac{2}{3}}\cos^2\theta + \frac{\sin^2\theta}{3}\left\{1 + \left(1-\gamma\right)^{\frac{1}{3}} + \left(1-\gamma\right)^{\frac{2}{3}}\right\}\right]. \tag{18}$$

This means that a constant μ rate is obtained by the XBS servo control that follows (18). In (18), force direction θ can be estimated from steer angle and vehicle velocity.

3.3 Deceleration servo control

The deceleration servo calculates the reference value of the pressure of the wheel cylinder in order to follow the reference of deceleration which calculates at XBS servo control. Since estimation of XBS uses the difference of frequency characteristics of wheel velocity shown in **Fig. 4**, the faster estimation than the break point frequency of the Wheel Deceleration Model (2-20 Hz) cannot be expected. This implies that estimation delay is too large to use in feedback control of wheel motion stabilization. Then, in this study, the control system structure with deceleration servo is adopted. The deceleration servo stabilizes wheel motion, and

follows reference value corresponding to the estimation value of XBS.

3.4 Brake servo control

The brake servo calculates the valve command of ABS in order to follow the reference of the pressure of the wheel cylinder calculating at deceleration servo control. The valve command of ABS is determined form difference between reference and measured pressure of the wheel cylinder as shown in **Table 1**.

Table 1 ABS valve control

Difference pressure	Valve control command
$P_b - P_{b0} > 2P_0$	Quick pressure reduction
$P_0 < P_b - P_{b0} \leq 2P_0$	Slow pressure reduction
$-P_0 < P_b - P_{b0} \leq P_0$	Hold
$-2P_0 < P_b - P_{b0} \leq -P_0$	Slow pressure build up
$P_b - P_{b0} \leq -2P_0$	Quick pressure build up

Here,

P_b : measured pressure of the wheel cylinder,

P_{b0}: reference value of pressure,

P_0 : threshold value of control.

Figure 8 shows frequency characteristics of the brake servo control. This figure shows that high cut off frequency characteristics are obtained by feedback control of the pressure of the wheel cylinder.

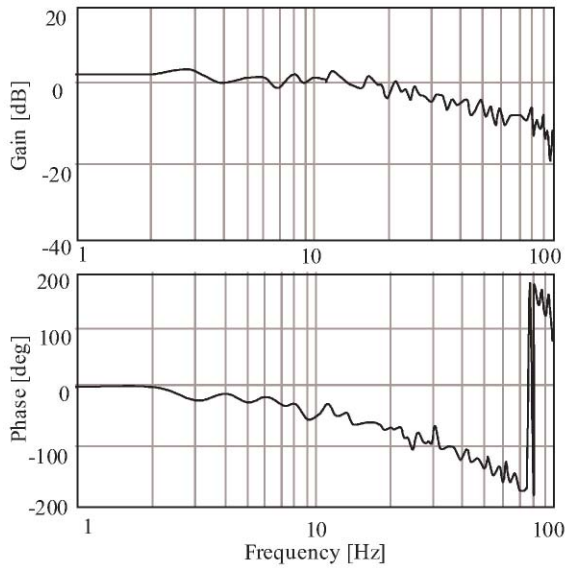

Fig. 8 Frequency characteristics of brake servo. (P_{b0} to P_b)

4. EXPERIMENTAL RESULTS

4.1 Braking on constant μ road

Figure 9 and **Figure 10** show experimental results of straight line braking on an artificial low friction road with the XBS servo which follows (18) and conventional ABS. Fluctuations of wheel velocity and the pressure of the wheel cylinder are suppressed by the XBS servo and a larger friction force is obtained than with conventional ABS.

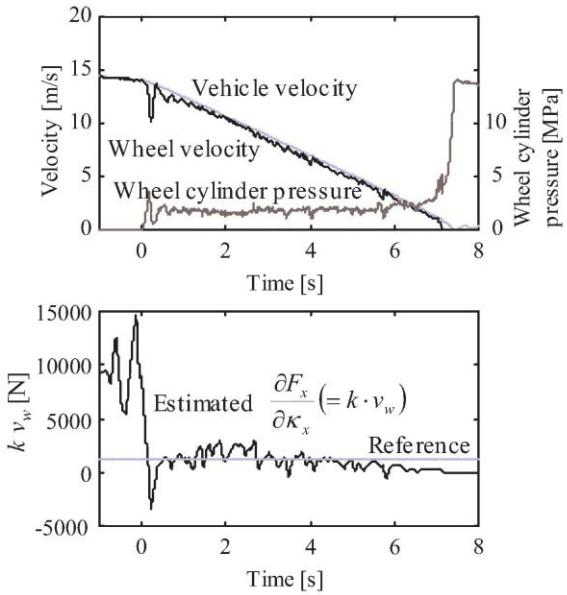

Fig. 9 Experimental results with XBS servo on artificial low friction road

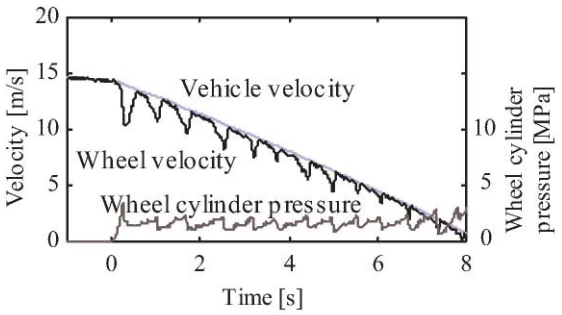

Fig. 10 Experimental results with conventional ABS on artificial low friction road

Figure 11 shows $F_x - \kappa_x$ plot, the approximated brush model and the operational point of the XBS servo on an artificial low friction road. In order to measure $F_x - \kappa_x$ plot, the wheel cylinder pressure of front wheels equipped with wheel dynamometers[6] increases at a constant rate until the front wheels are locked.[7] Vehicle velocity is also measured by optical sensor, and κ_x is

calculated by (8). The parameters K_s and μ of the brush model (12) are decided so that the model approximates to $F_x - \kappa_x$ plot. The operational point of the XBS servo indicates average F_x and κ_x during XBS servo operation (experimental result shown in **Fig. 9**). Each experiment, i. e. measurement of friction force characteristics and the XBS servo, has the same initial velocity of 15 m/s. **Figure 11** also shows average value of $\partial F_x / \partial \kappa_x$ calculated by multiplying the estimated XBS by vw. This figure shows that desirable friction force can be obtained by the XBS servo.

The effect of the XBS servo during combined steering and braking maneuvers is shown in **Fig. 12**. The brake is applied on vehicles turning with a constant steering wheel angle on an artificial low friction road from an initial velocity of 15 m/s, and the longitudinal and lateral forces of the front wheels are measured by wheel dynamometers. **Figure 12** shows the average longitudinal friction coefficient ($\mu_x = F_x / F_z$) and the lateral friction coefficient ($\mu_y = F_y / F_z$) for 2 seconds from applying the brake.

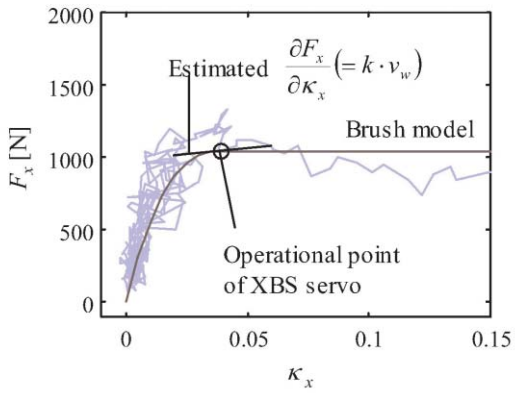

Fig. 11 Friction force characteristics on artificial low friction road

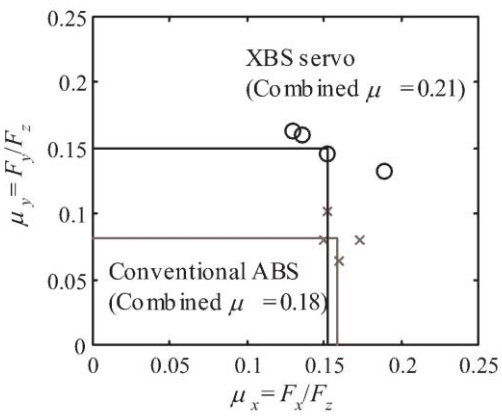

Fig. 12 Friction force characteristics on artificial low friction road

The points O and X indicate four experimental results of the XBS servo and conventional ABS, respectively. This figure shows that combined μ $\left(=\sqrt{\mu_x{}^2 + \mu_y{}^2}\right)$ is also improved by the XBS servo.

4.2 Adaptation to change of road friction characteristics

XBS servo avails a μ peak following control even if maximum friction coefficient μ changes. In this section, we evaluate the adaptation of the XBS servo to changes in road friction characteristics. **Figure 13** shows the experimental results of the XBS servo during changes in road friction characteristics from an artificial low friction road to a dry road.

When the vehicle transitions from an artificial low friction road to a dry road, estimated $\partial F_x / \partial \kappa_x$ increases according to the increase in the margin of friction force. Then, the XBS servo works to increase wheel cylinder pressure more rapidly than conventional ABS, as shown in **Fig. 14**.

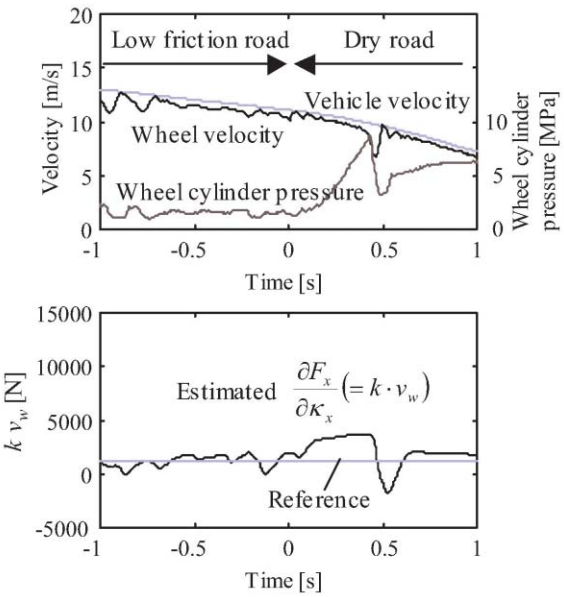

Fig. 13 Experimental results of XBS servo during change of road friction characteristics from artificial low friction road to dry road

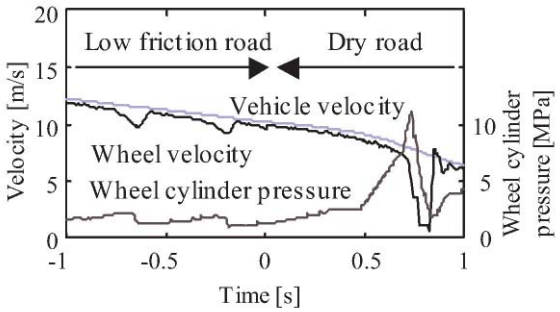

Fig. 14 Experimental results of conventional ABS during changes in road friction characteristics from artificial low friction road to dry road

5. CONCLUSION

XBS is an important parameter in identifying tire/road friction characteristics. In this paper, the estimation method of XBS is proposed and the performance of the XBS estimation is experimentally verified. Furthermore, we demonstrate the XBS servo control, which obtains a constant μ rate, as compared with conventional ABS. In the future, we expect that XBS can be applied for brake control systems, e.g. Electro Hydraulic Brake EHB[8) 9)] and Electro Mechanical Brake EMB,[10)] to greatly enhance vehicle control performance.

REFERENCES

1) Ono, E. and S. Hosoe, "Techniques in vehicle integrated control for steering and traction systems". In: Mechatronic systems techniques and applications: Volume 2 Transportation and vehicular systems (Leondes, C. T. (Ed)), pp. 99-149. Gordon and Breach Science Publishers, 2000.

2) Bernard, J. E., L. Segel and R. E. Wild, "Tire shear force generation during combined steering and braking maneuvers", SAE paper, 1977, 770852.

3) Bakker, E., L. Nyborg and H. B. Pacejka, "Tyre modelling for use in vehicle dynamics studies", SAE paper, 1987, 870421.

4) Umeno, T., E. Ono, K. Asano, A. Tanaka, S. Ito, Y. Yasui and M. Sawada, "Estimation of tire-road friction using tire vibration model", SAE paper., 2002, 2002-01-1183.

5) Ljung, L, "System Identification, Theory for the user", 1987, pp. 305-311, Prentice-Hall.

6) Burkard, H. and C. Calame, "Rotating wheel dynamometer with high frequency response". Tire Technology International 1998, pp. 154-158, 1998

7) Yasui, Y., H. Nitta, T. Yoshida, T. Hosome and K. Kawamura, "Experimental approach for evaluating tire characteristics and ABS performance". SAE paper, 2000, 2000-01-0110.

8) Jonner, W. D., H. Winner, L. Dreilich and E. Schunck, "Electrohydraulic brake system, The first approach to brake-by-wire technology". SAE paper, 1996, 960991.

9) Leffler, H., "Electronic brake management EBM, Prospects of an integration of brake system and driving stability control", SAE paper, 1996, 960954.

10) Maron, C., T. Dieckmann, S. Hauck and H. Prinzler, "Electromechanical brake system, Actuator control development system". SAE paper, 1997, 970814.

＜著　者＞

沢田　護
（さわだ　まもる）

安全走行事業部
車両制御開発業務に従事

小野　英一
（おの　えいいち）

(株)豊田中央研究所 車両制御研究室
工学博士
車両運動制御，状態推定業務に従事

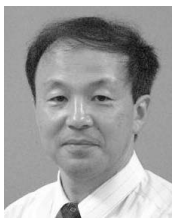

浅野　勝宏
（あさの　かつひろ）

(株)豊田中央研究所 車両制御研究室
工学博士
モータ制御、電力変換、車両状態推定・制御業務に従事

菅井　賢
（すがい　まさる）

(株)豊田中央研究所 車両制御研究室
車両状態推定・制御、モータ制御業務に従事

伊藤　祥司
（いとう　しょうじ）

トヨタ自動車(株)　統合システム開発部
車両制御関係業務に従事

山本　真規
（やまもと　まさみ）

トヨタ自動車(株)　第2車両技術部
車両制御関係業務に従事

安井　由行
（やすい　よしゆき）

アイシン精機(株)　走行系技術部
制御サスペンションの開発に従事